

Spacetime with off-diagonal stress

Inyong Cho^{*} and Rajibul Shaikh[†]

Institute of Convergence Fundamental Studies,

School of Natural Sciences, College of Liberal Arts,

Seoul National University of Science and Technology, Seoul 01811, Korea

Abstract

We investigate the evolution of spacetime driven by matter fluid with off-diagonal stress components in the energy-momentum tensor. The off-diagonal stress components require nonzero shear viscosity of fluid. We consider the simplest form of the equation of state for fluid, for which the pressure and the off-diagonal stress are proportional to the energy density individually. The spacetime evolution exhibits an anisotropic expansion due to the off-diagonal shear viscosity. At late times, compared with the usual Friedmann universe, we find that the Universe expands less rapidly as the energy density drops faster due to the transfer to the stress. For some ranges of the equation-of-state parameters, we find that the initial big-bang singularity can be removed.

arXiv:2209.12544v2 [gr-qc] 8 Dec 2022

^{*} iycho@seoultech.ac.kr

[†] rajibulsk@gmail.com

I. INTRODUCTION

It is well known how the Friedmann universe evolves with perfect fluid, in particular, barotropic fluid. With the energy-momentum tensor,

$$T_{\nu}^{\mu} = \text{diag}[-\rho, p, p, p], \quad (1)$$

of which the equation of state is given by $p = w\rho$, and with the metric ansatz,

$$ds^2 = -dt^2 + a^2(t) (dx^2 + dy^2 + dz^2), \quad (2)$$

the solutions to the Einstein's equation provides the scale factor, the energy density, and the three-volume density as (for $w > -1$)

$$a = a_0 t^{2/[3(1+w)]}, \quad (3)$$

$$\rho = \rho_0 a^{-3(1+w)} \propto \frac{1}{t^2}, \quad (4)$$

$$\mathcal{V}_3 \equiv \sqrt{g^{(3)}} = a^3 = a_0^3 t^{2/(1+w)}. \quad (5)$$

However, the Friedmann universe with the off-diagonal stress components (T_j^i) of fluid has not been studied well. There are a few trials considering these components in fluid dynamics [1–3], but not in the scope of spacetime structure. In this paper, we consider the fluid of which the energy-momentum tensor contains the off-diagonal stress terms in addition to the diagonal terms.

The physical meaning of T^{ij} is the j -component of flux of i -component of momentum, or i -component of force produced by matter at $x^j - \epsilon$ acting on matter at $x^j + \epsilon$ across a unit surface, perpendicular to which is \hat{e}_j [3]. This type of stress component may arise in the cosmological perturbations when both the scalar and the tensor modes are introduced. In particular, it appears in the effective energy-momentum tensor composed of the quadratic terms of the coupled linear scalar and tensor modes.

In Eckart's theory, the energy-momentum tensor of fluid with heat flow and viscosity is given by [3]

$$T^{\mu\nu} = \rho u^{\mu} u^{\nu} + (p - \xi\Theta)h^{\mu\nu} + q^{\mu} u^{\nu} + q^{\nu} u^{\mu} - 2\eta\sigma^{\mu\nu}. \quad (6)$$

Here, $\xi(> 0)$ and $\eta(> 0)$ are the bulk and the shear viscosities, q^{μ} is the heat-flux four-vector, u^{μ} is the four-velocity of fluid, $h_{\mu\nu} = g_{\mu\nu} + u_{\mu}u_{\nu}$ is the projection tensor, $\Theta = u^{\mu}_{;\mu}$ is the expansion, and $\sigma_{\mu\nu} = (u_{\mu;\delta}h_{\nu}^{\delta} + u_{\nu;\delta}h_{\mu}^{\delta})/2 - \Theta h_{\mu\nu}/3$ is the symmetric traceless shear tensor of fluid. The above energy-momentum tensor can be written down as the sum of three components: the perfect-fluid component $T_{\text{pf}}^{\mu\nu} = \rho u^{\mu} u^{\nu} + p h^{\mu\nu}$, the heat-flux component $T_{\text{heat}}^{\mu\nu} = q^{\mu} u^{\nu} + q^{\nu} u^{\mu}$, and the viscosity component $T_{\text{visc}}^{\mu\nu} = -\xi\Theta h^{\mu\nu} - 2\eta\sigma^{\mu\nu}$.

In this work, we would like to investigate the effect of the *off-diagonal shear viscosity*. To do that, we consider the perfect fluid with only the off-diagonal shear-viscosity components ($\eta \neq 0$, $\xi = 0$, and $q^{\mu} = 0$).

Cosmology with the shear viscosity, in addition to the perfect fluid, has been explored in the literature in Refs. [4–9]. In these models, only the *diagonal* shear viscosity was considered, and the metric was modelled either by the Friedmann-Robertson-Walker (FRW) type [4], or by the Bianchi type [5–9]. However, in this work, we shall consider the off-diagonal shear viscosity, and investigate its cosmological effects with a non-diagonal metric.

II. MODEL AND FIELD EQUATIONS

Let us consider the fluid of which the energy-momentum tensor is given by

$$T_{\nu}^{\mu} = \begin{bmatrix} -\rho & 0 & 0 & 0 \\ 0 & p & \sigma & \sigma \\ 0 & \sigma & p & \sigma \\ 0 & \sigma & \sigma & p \end{bmatrix}, \quad (7)$$

where the energy density ρ , the pressure p , and the stress σ depend only on time t . We adopt a metric ansatz which has off-diagonal components,

$$\begin{aligned} ds^2 &= -dt^2 + a^2(t) (dx^2 + dy^2 + dz^2) + 2b(t) (dxdy + dydz + dzdx) \\ &= -dt^2 + \frac{1}{3} [2c^2(t) + d^2(t)] (dx^2 + dy^2 + dz^2) + \frac{2}{3} [d^2(t) - c^2(t)] (dxdy + dydz + dzdx), \end{aligned} \quad (8)$$

where we rewrote the metric (8) to (9) by $a^2 = (2c^2 + d^2)/3$ and $b = (d^2 - c^2)/3$. Later we shall see that it is easier to solve the field equations with the metric (9). In addition, the three-volume density is given simply by $\mathcal{V}_3 = (a^2 - b)\sqrt{a^2 + 2b} = c^2 d$. For the fluid four-velocity $u^\mu = (u^t, u^x, u^y, u^z) = (1, 0, 0, 0)$, the expansion and the nonzero components of the shear tensor become $\Theta = 2\dot{c}/c + \dot{d}/d$ and $\sigma_j^i (i \neq j) = -(\dot{c}/c - \dot{d}/d)/3$. Then, the energy-momentum tensor (7) can be put into the form (6) for $\eta \neq 0$, $\xi = 0$, and $q^\mu = 0$, with $\sigma = 2\eta(\dot{c}/c - \dot{d}/d)/3$.

The three dimensional (3D) sector (t -constant hypersurface) of the metric (8) has the maximum number of Killing vectors (six for 3D space), and the induced Riemannian metric $h_{\mu\nu} = g_{\mu\nu} + u_\mu u_\nu$ exhibits vanishing 3D Riemann curvature tensor on the hypersurface. This indicates that the spatial sector of our metric is so called *maximally symmetric*, and the 3D space is homogeneous and isotropic [10, 11] similar to the *flat* FRW metric.

Although the 3D space exhibits the isotropy, the evolution of the spacetime is *anisotropic*. By coordinate transformations,

$$X = \frac{1}{\sqrt{2}}(-x + z), \quad Y = \frac{1}{\sqrt{6}}(-x + 2y - z), \quad Z = \frac{1}{\sqrt{3}}(x + y + z), \quad (10)$$

the metric (9) can be transformed to the Bianchi type VII metric,

$$ds^2 = -dt^2 + c^2(t)(dX^2 + dY^2) + d^2(t)dZ^2, \quad (11)$$

and the energy-momentum tensor (7) is transformed to

$$T_\nu^\mu = \text{diag}[-\rho, p - \sigma, p - \sigma, p + 2\sigma]. \quad (12)$$

Solving the Einstein's equation with the diagonal metric (11) and the energy-momentum tensor (12) is equivalent to solving with the off-diagonal ones, Eqs. (9) and (7).¹

The components of the Einstein's equation $G_\nu^\mu = T_\nu^\mu$ ($c = 1, 8\pi G = 1$) give

$$\rho = \frac{\dot{c}(d\dot{c} + 2c\dot{d})}{c^2d}, \quad (13)$$

$$p = -\frac{d(\dot{c}^2 + 4c\ddot{c}) + 2c(\dot{c}\dot{d} + c\ddot{d})}{3c^2d}, \quad (14)$$

$$\sigma = -\frac{d(\dot{c}^2 + c\ddot{c}) - c(\dot{c}\dot{d} + c\ddot{d})}{3c^2d}. \quad (15)$$

In order to solve these field equations, we introduce two equations of state,

$$p = \alpha\rho, \quad \sigma = \beta\rho. \quad (16)$$

With Eqs. (16) and (13), Eqs. (14) and (15) can be written as

$$2cd\ddot{c} + \frac{1+3\alpha}{2}d\dot{c}^2 + (1+3\alpha)c\dot{c}\dot{d} + c^2\ddot{d} = 0, \quad (17)$$

$$cd\ddot{c} + (1+3\beta)d\dot{c}^2 - (1-6\beta)c\dot{c}\dot{d} - c^2\ddot{d} = 0. \quad (18)$$

The addition of these equations (17) and (18) gives

$$\frac{\ddot{c}}{\dot{c}} + \frac{1+\alpha+2\beta}{2}\frac{\dot{c}}{c} + (\alpha+2\beta)\frac{\dot{d}}{d} = 0, \quad (19)$$

which can be integrated to give

$$c^{(1+\alpha+2\beta)/2}d^{\alpha+2\beta}\dot{c} = A_1 \quad : \text{c-equation}, \quad (20)$$

where A_1 is an integration constant. Subtraction of Eq. (18) from Eq. (17) gives

$$2cd\ddot{c} + (-1+3\alpha-6\beta)d\dot{c}^2 + 2(2+3\alpha-6\beta)c\dot{c}\dot{d} + 4c^2\ddot{d} = 0, \quad (21)$$

which can be rewritten as

$$\frac{d}{dt} \left[c^{(-1+3\alpha-6\beta)/2}(d\dot{c} + 2c\dot{d}) \right] = 0. \quad (22)$$

¹ The physical meaning of the scale factors c and d are understood better in the diagonal metric (11), while that of the pressure p and the off-diagonal shear stress σ are understood better in the off-diagonal energy-momentum tensor (7).

Integrating this equation, we have

$$c^{(-1+3\alpha-6\beta)/2}(d\dot{c} + 2cd) = A_2, \quad (23)$$

where A_2 is an integration constant. Using Eq. (20), this finally reduces to

$$2c^{(1+3\alpha-6\beta)/2}\dot{d} = A_2 - A_1 \frac{d^{1-\alpha-2\beta}}{c^{1-\alpha+4\beta}} \quad : d\text{-equation.} \quad (24)$$

Using c - and d -equation in Eqs. (20) and (23), we obtain the energy density from Eq. (13),

$$\rho = \frac{A_1 A_2}{c^{2(1+\alpha-\beta)} d^{1+\alpha+2\beta}} \quad : \rho\text{-solution.} \quad (25)$$

Note that A_1 and A_2 must have the same sign to make ρ positive.

In this section, we manipulated the field equations and obtained the equations in simple forms; the c -equation (20) and the d -equation (24) which are the first-order differential equations, and the energy density (25) in a closed form.

III. SOLUTIONS

In this section, we solve the field equations obtained earlier. We present the general and special classes depending on the values of the equation-of-state parameters, α and β . Dividing the the d -equation (24) by the c -equation (20), we have

$$2 \frac{c^{\alpha-4\beta} \dot{d}}{d^{\alpha+2\beta} \dot{c}} = \frac{A_2}{A_1} - \frac{d^{1-\alpha-2\beta}}{c^{1-\alpha+4\beta}}. \quad (26)$$

Defining $x \equiv c^{1-\alpha+4\beta}$ and $y \equiv d^{1-\alpha-2\beta}$, this equation can be written as

$$\frac{d}{dt} (x^m y) = \frac{A_2}{A_1} m x^m \dot{x}, \quad (27)$$

where $m = (1 - \alpha - 2\beta)/[2(1 - \alpha + 4\beta)]$.

Class G: general class

Equation (27) is integrated to give d as a function of c ,

$$d = \frac{1}{\sqrt{c}} \left[\frac{A_2}{3A_1} \frac{1-\alpha-2\beta}{1-\alpha+2\beta} c^{3(1-\alpha+2\beta)/2} + A_3 \right]^{\frac{1}{1-\alpha-2\beta}} \quad : d\text{-solution,} \quad (28)$$

where A_3 is an integration constant. Then plugging this expression for d in the c -equation (20), we get c in an implicit integral form,

$$t = \frac{1}{A_1} \int_{c_0}^c \sqrt{c} \left[\frac{A_2}{3A_1} \frac{1-\alpha-2\beta}{1-\alpha+2\beta} c^{3(1-\alpha+2\beta)/2} + A_3 \right]^{\frac{\alpha+2\beta}{1-\alpha-2\beta}} dc \quad : c\text{-solution,} \quad (29)$$

where $c_0 = c(t = 0)$. The integration can be performed numerically to obtain c , and we show the result in the next section. Now the solutions for c , d and ρ can be fully obtained from Eqs. (29), (28) and (25).

There are three classes for which Eq. (27) can not be used, so the d - and c -solutions, (28) and (29), are not valid; $1 - \alpha + 2\beta = 0$ ($m = -1$), $1 - \alpha - 2\beta = 0$ ($y = 1$), and $1 - \alpha + 4\beta = 0$ ($x = 1$). These classes need to be treated separately.

Class A: $1 - \alpha + 2\beta = 0$ ($\alpha \neq 1$ and $\beta \neq 0$)²

This class corresponds to $m = -1$. Integrating Eq. (27), we get

$$d = \frac{1}{\sqrt{c}} \left[\frac{A_2}{A_1} (1 - \alpha) \log c + A_{3A} \right]^{\frac{1}{2(1-\alpha)}}, \quad (30)$$

where A_{3A} is an integration constant. Plugging this in the c -equation (20), we get

$$t = \frac{1}{A_1} \int_{c_0}^c \sqrt{c} \left[\frac{A_2}{A_1} (1 - \alpha) \log c + A_{3A} \right]^{\frac{2\alpha-1}{2(1-\alpha)}} dc. \quad (31)$$

Class B: $1 - \alpha - 2\beta = 0$ ($\alpha \neq 1$ and $\beta \neq 0$)

For this class, Eq. (26) becomes

$$2 \frac{\dot{d}}{d} = \frac{A_2}{A_1} \frac{\dot{c}}{c^{3\alpha-2}} - \frac{\dot{c}}{c}, \quad (32)$$

and the solution is given by

$$d = \frac{A_{3B}}{\sqrt{c}} \exp \left[\frac{A_2}{6(1-\alpha)A_1} c^{3(1-\alpha)} \right], \quad (33)$$

where A_{3B} is an integration constant. Plugging this in the c -equation (20), we get

$$t = \frac{A_{3B}}{A_1} \int_{c_0}^c \sqrt{c} \exp \left[\frac{A_2}{6(1-\alpha)A_1} c^{3(1-\alpha)} \right] dc. \quad (34)$$

Class C: $1 - \alpha + 4\beta = 0$ ($\alpha \neq 1$ and $\beta \neq 0$)

For this class, Eq. (26) becomes

$$\frac{2d^{(1-3\alpha)/2} \dot{d}}{A_2/A_1 - d^{3(1-\alpha)/2}} = \frac{\dot{c}}{c}, \quad (35)$$

and the solution is given by

$$d = \left[\frac{A_2}{A_1} - A_{3C} c^{-3(1-\alpha)/4} \right]^{\frac{2}{3(1-\alpha)}}, \quad (36)$$

² If $\alpha = 1$, $\beta = 0$, which is the stress-free case. It will be dealt with in Class D.

where A_{3C} is an integration constant. Plugging this in the c -equation (20), we get

$$t = \frac{1}{A_1} \int_{c_0}^c c^{(3\alpha+1)/4} \left[\frac{A_2}{A_1} - A_{3C} c^{-3(1-\alpha)/4} \right]^{\frac{3\alpha-1}{3(1-\alpha)}} dc. \quad (37)$$

Class D: $\beta = 0$

This is the class for which the off-diagonal stress terms are *absent*, i.e., $T_j^i(i \neq j) = 0$. The usual Friedmann universe belongs to this class. This case is described by the general c -, d - and ρ -solutions, Eqs. (29), (28) and (25). We need to treat separately for $\alpha = 1$ and $\alpha \neq 1$. Integrating Eq. (26), we get

$$d = \begin{cases} A_{3D} c^{(A_2 - A_1)/(2A_1)} & (\alpha = 1) \\ \frac{1}{\sqrt{c}} \left[\frac{A_2}{3A_1} c^{3(1-\alpha)/2} + A_{3D} \right]^{\frac{1}{1-\alpha}} & (\alpha \neq 1) \end{cases}, \quad (38)$$

where A_{3D} is an integration constant. Plugging this in the c -equation (20), we get

$$A_1 t + A_4 = \begin{cases} \frac{2A_1 A_{3D}}{3A_1 + A_2} c^{(3A_1 + A_2)/(2A_1)} & (\alpha = 1) \\ \int \sqrt{c} \left[\frac{A_2}{3A_1} c^{3(1-\alpha)/2} + A_{3D} \right]^{\frac{\alpha}{1-\alpha}} dc & (\alpha \neq 1) \end{cases}, \quad (39)$$

where A_4 is an integration constant.

(i) FRW universe: Although the energy-momentum tensor is diagonal in this case, the metric is not since $c \neq d$ in general. The metric becomes diagonal and reduces to that of the usual Friedmann-Robertson-Walker universe when $c = d$. This can be achieved by setting the conditions at a certain time, say at $t = 0$, $c = d$ and $\dot{c} = \dot{d}$. Applying these conditions on Eq. (38) at $t = 0$, we find the integration constants, $A_2 = 3A_1$, and $A_{3D} = 1$ for $\alpha = 1$ and $A_{3D} = 0$ for $\alpha \neq 1$. From Eq. (39) with these constants, we obtain

$$c = d = \begin{cases} e^{(A_1 t + A_4)} & (\alpha = -1) \\ \left[\frac{3(1+\alpha)}{2} (A_1 t + A_4) \right]^{\frac{2}{3(1+\alpha)}} & (\alpha \neq -1) \end{cases}, \quad (40)$$

which makes the metric diagonal. If we restrict the conditions further, $c(0) = c_0 = 1$, without loss of generality, we get $A_4 = 0$ for $\alpha = -1$ and $A_4 = 2/[3(1+\alpha)]$ for $\alpha \neq -1$.

(ii) Non-FRW universe: In Sec. II, it was noted that the shear tensor is given by $\sigma_j^i(i \neq j) = -(\dot{c}/c - \dot{d}/d)/3$. Therefore, for the diagonal (FRW) metric in Class (i), the shear tensor vanished identically representing shear-free cosmology. However, if we do not impose the conditions $c = d$ and $\dot{c} = \dot{d}$ at $t = 0$, the off-diagonal components of the metric are nonzero, and the solutions are given by Eqs. (38) and (39). For this class, the energy-momentum tensor is diagonal, $T_j^i(i \neq j) = 0$, while the shear tensor is nonzero, $\sigma_j^i(i \neq j) \neq 0$. We shall not pay much attention to this non-FRW class in what follows.³

³ Note that for $\alpha = 1$ with an appropriate rescaling, we have $c = t^{p_1}$ and $d = t^{p_3}$, where $p_1 = 2A_1/(3A_1 + A_2)$ and $p_3 = (A_2 - A_1)/(3A_1 + A_2)$. This is a Kasner-type solution in nonvacuum.

Kasner type

There exists an off-diagonal metric solution for the vacuum which is a Kasner-type. From Eqs. (23) and (25), if $A_2 = 0$, we have $\rho = 0$ (i.e., $p = \sigma = 0$) and $d = B_1/\sqrt{c}$. From Eq. (20), we get $c = (B_2t + B_3)^{2/3}$, where B_i 's are constants. The volume density $\mathcal{V}_3 = B_1(B_2t + B_3)$ becomes zero at the initial moment $t_s = -B_3/B_2$ at which the Kretschmann scalar $\mathcal{K} = 64B_2^4/[27(B_2t + B_3)^4]$ diverges. Seen from the diagonal Bianchi-type metric (11), we have $c = t^{p_1}$ and $d = t^{p_3}$, where $p_1 = 2/3$ and $p_3 = -1/3$, after rescaling time and setting $B_1 = 1$. This is nothing but the vacuum Kasner solution [12, 13].

IV. SOLUTIONS AND EFFECT OF STRESS

In this section, we present the numerical solutions and discuss the effect of the stress σ by comparing with the stress-free case ($\beta = 0$). We integrate the c -solution in Eq. (29) [Eqs. (31), (34), (37), and (39) for special cases]. Then d is obtained from Eq. (28) [Eqs. (30), (33), (36), and (38) for special cases], and ρ is obtained from Eq. (25).

The integration constants are determined by imposing the initial conditions. Since the original field equations are the second-order differential equations for c and d , we have four integration constants, c_0 and three A_i 's. In order to compare with the usual Friedmann universe ($\beta = 0$), we impose the initial conditions in the same way as discussed in Sec. III.

At $t = 0$, we impose three conditions, $c(0) = d(0) = 1$ and $\dot{c}(0) = \dot{d}(0)$. Then $c_0 \equiv c(0) = 1$. We get $A_2/A_1 = 3$ from Eq. (26), and A_{3i} is obtained from Eq. (28) [Eqs. (30), (33), (36), and (38) for special cases]. Fixing the value of $\dot{c}(0)$ in Eq. (20) determines the remaining freedom A_1 .

We integrate the c -solution in both directions in t from $t = 0$. In Fig. 1, we plotted the numerical results of the metric functions c and d , the three-volume density \mathcal{V}_3 , the energy density ρ , and the Kretschmann scalar \mathcal{K} . We presented the results for the values of the equation-of-state parameters, $\alpha, \beta = 0, \pm 1/3, \pm 1$. The green lines correspond to the usual Friedmann universe ($\beta = 0$: stress-free).

A. Metric functions c and d , and three-volume density \mathcal{V}_3

For the usual Friedmann universe ($\beta = 0$: green lines in Fig. 1) the metric functions c and d becomes $c = d = a$. The functional form of the scale factor $a(t)$ is given similarly by Eq. (3) for $\alpha > -1$, for which the big-bang singularity exists,

$$a(t) = a_0(t - t_s)^{2/[3(1+\alpha)]}, \quad (41)$$

where t_s is the moment of big bang (the moment of the three-volume density \mathcal{V}_3 vanishes in our numerical calculations). For $\alpha = -1$, the scale factor becomes that of de Sitter space and $t_s \rightarrow -\infty$.

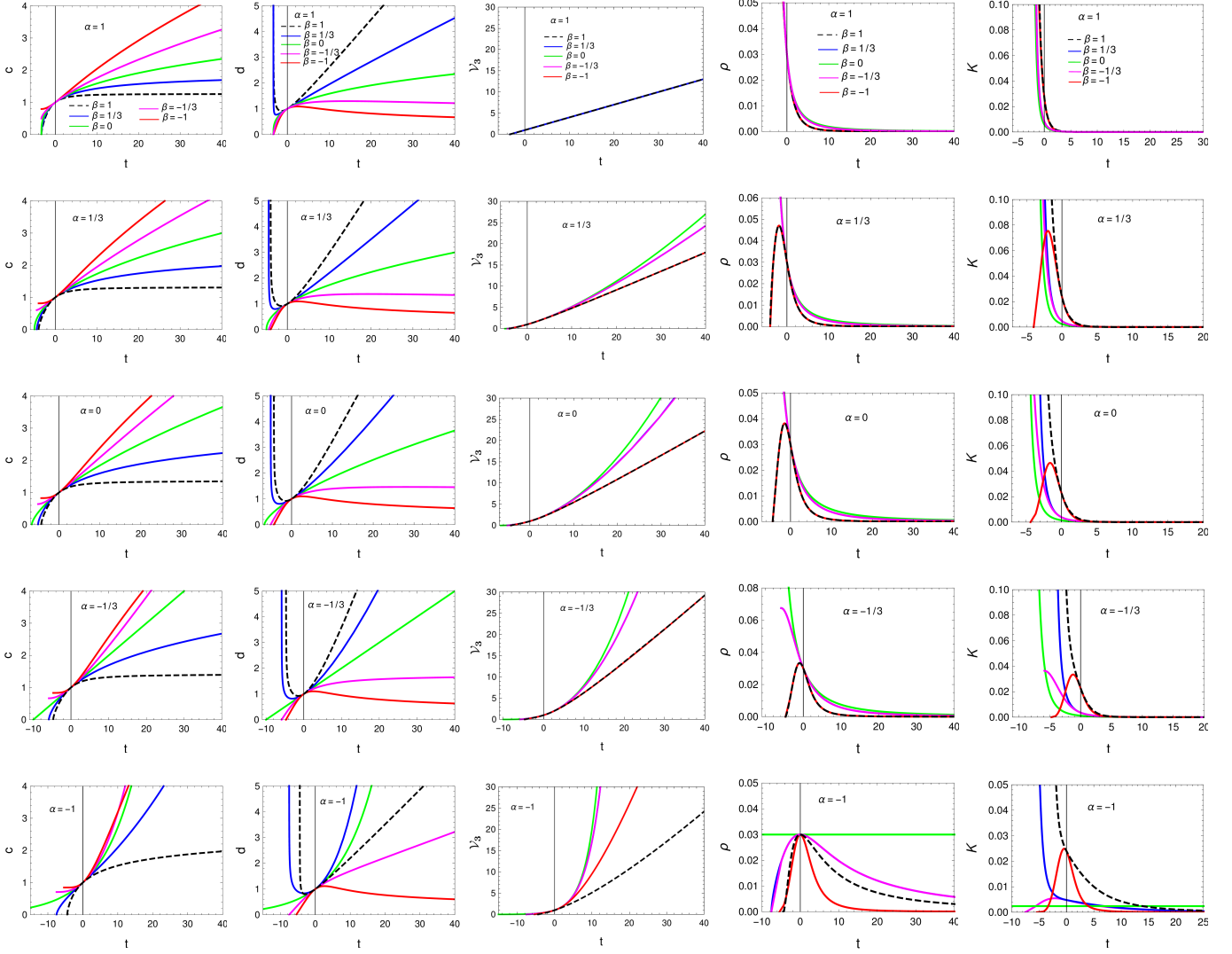


FIG. 1. Plots of c , d , \mathcal{V}_3 , ρ and \mathcal{K} for $\alpha, \beta = 0, \pm 1/3, \pm 1$. Plots in a given row are for the same value of α . Different values of β are distinguished by the line color.

If $\beta \neq 0$, the metric functions c and d evolve in a different way, which exhibits an anisotropy (we shall discuss this anisotropy more in detail in Sec. VI.) For $\beta > 0$, as $t \rightarrow t_s$, the metric function c goes to zero and d diverges. This means that c and d exhibit an expansion and a contraction individually. For $\beta < 0$, as $t \rightarrow t_s$, c goes to a nonzero value and d goes to zero. Both c and d exhibit an expansion. Although the metric functions c and d behave oppositely as $t \rightarrow t_s$, the three-volume density \mathcal{V}_3 vanishes at $t \rightarrow t_s$, which exhibits the big bang at the initial moment. [This is true for all the cases except for de Sitter, $(\alpha, \beta) = (-1, 0)$.] \mathcal{V}_3 increases in time monotonically.

B. Energy density ρ

For the usual Friedmann universe ($\beta = 0$), the energy density ρ is given similarly by Eq. (4) for $\alpha > -1$. It decreases monotonically in t and diverges at the moment of big bang ($t \rightarrow t_s$). It remains constant in time for the de Sitter space $\alpha = -1$.

For $\beta \neq 0$, however, there are some cases which are different from the conventional Friedmann universe. In Fig. 1, we observe some cases for which ρ increases in t at the early stage. In addition, as summarized in Tab. I, there are several cases for which the energy density does not diverge at the initial moment, $\rho(t \rightarrow t_s) \nrightarrow \infty$.

C. Kretschmann scalar \mathcal{K}

In the previous subsections, we observed that the three-volume density \mathcal{V}_3 vanishes at $t = t_s$ except for the de Sitter space $[(\alpha, \beta) = (-1, 0)]$ while the energy density ρ does not necessarily diverge. Therefore, it is better to evaluate the curvature to examine the character of the spacetime. The Kretschmann scalar is given by

$$\mathcal{K} = R^{\mu\nu\rho\sigma} R_{\mu\nu\rho\sigma} = \frac{12A_1^4}{c^{6+2\alpha+4\beta}d^{4\alpha+8\beta}} + \frac{(3\alpha^2 + 24\beta^2 + 2\alpha - 8\beta + 3)A_1^2A_2^2}{c^{4+4\alpha-4\beta}d^{2+2\alpha+4\beta}} + \frac{8(3\beta - 1)A_1^3A_2}{c^{5+3\alpha}d^{1+3\alpha+6\beta}}. \quad (42)$$

We plotted \mathcal{K} in Fig. 1, and presented its value at $t = t_s$ in Tab. I. There are three classes in the relation between ρ and \mathcal{K} at t_s ;

- (i) for $\rho = \infty$, (A) $\mathcal{K} = \infty$,
- (ii) for $\rho = 0$, (A) $\mathcal{K} = \infty$ or (B) 0,
- (iii) for $\rho = \text{constant}$, (A) $\mathcal{K} = \infty$ or (C) constant.

Regarding $\mathcal{V}_3(t_s) = 0$, most of the classes are acceptable except (iii-C) for which the spacetime is regular while the energy density remains finite with zero volume. There are possibilities of avoiding the big-bang singularity for (ii-B) $[(\alpha, \beta) = (1/3, -1), (0, -1), (-1/3, -1), (-1, -1/3), (-1, -1)]$, and (iii-C) $[(\alpha, \beta) = -1/3, -1/3]$. In particular, it is interesting that for the radiation- and the matter-dominated epochs, the big-bang singularity can be removed if the shear is $\sigma = -\rho$, i.e., $(\alpha, \beta) = (1/3, -1), (0, -1)$.

D. $\rho(t_s)$ & $\mathcal{K}(t_s)$

Let us discuss the initial singularity more in detail. We investigate the solutions in the limit of $t \rightarrow t_s$ in order to inspect the behaviour of $\rho(t_s)$ and $\mathcal{K}(t_s)$. At $t = 0$, we imposed the initial conditions, $c(0) = d(0) = 1$ and $\dot{c}(0) = \dot{d}(0)$. They give $A_2 = 3A_1$ from Eq. (26) and $A_3 = 4\beta/(1 - \alpha + 2\beta)$ from Eq. (28). Considering the signatures of the terms in the integrand, the c -solution for Class G in Eq. (29) is classified into four

TABLE I. Energy density ρ and Kretschmann scalar \mathcal{K} at t_s

α	β	$\rho(t_s)$	$\mathcal{K}(t_s)$	Nature
1	$1, \frac{1}{3}, 0, -\frac{1}{3}, -1$	∞	∞	singular
$\frac{1}{3}$	1	0	∞	singular
	$\frac{1}{3}, 0, -\frac{1}{3}$	∞	∞	singular
	-1	0	0	regular
0	1	0	∞	singular
	$\frac{1}{3}, 0, -\frac{1}{3}$	∞	∞	singular
	-1	0	0	regular
$-\frac{1}{3}$	1	0	∞	singular
	$\frac{1}{3}$	const.	∞	singular
	0	∞	∞	singular
	$-\frac{1}{3}$	const.	const.	regular
	-1	0	0	regular
-1	$1, \frac{1}{3}$	0	∞	singular
	0	const.	const.	regular
	$-\frac{1}{3}, -1$	0	0	regular

cases,

$$t = \begin{cases} \frac{1}{A_1} \int_1^c \sqrt{c} \left[\frac{1-\alpha-2\beta}{1-\alpha+2\beta} \left(c^{3(1-\alpha+2\beta)/2} - c_*^{3(1-\alpha+2\beta)/2} \right) \right]^{\frac{\alpha+2\beta}{1-\alpha-2\beta}} dc & \text{(G1: } \beta < 0 \text{ \& } 1 - \alpha + 2\beta > 0) \\ \frac{1}{A_1} \int_1^c \sqrt{c} \left[\frac{1-\alpha-2\beta}{|1-\alpha+2\beta|} \left(-c^{-3|1-\alpha+2\beta|/2} + c_*^{-3|1-\alpha+2\beta|/2} \right) \right]^{\frac{\alpha+2\beta}{1-\alpha-2\beta}} dc & \text{(G2: } \beta < 0 \text{ \& } 1 - \alpha + 2\beta < 0) \\ \frac{1}{A_1} \int_1^c \sqrt{c} \left[\frac{1-\alpha-2\beta}{1-\alpha+2\beta} \left(c^{3(1-\alpha+2\beta)/2} + c_*^{3(1-\alpha+2\beta)/2} \right) \right]^{\frac{\alpha+2\beta}{1-\alpha-2\beta}} dc & \text{(G3: } \beta > 0 \text{ \& } 1 - \alpha - 2\beta > 0) \\ \frac{1}{A_1} \int_1^c \sqrt{c} \left[\frac{1-\alpha-2\beta}{1-\alpha+2\beta} \left(-c^{3(1-\alpha+2\beta)/2} + c_*^{3(1-\alpha+2\beta)/2} \right) \right]^{\frac{\alpha+2\beta}{1-\alpha-2\beta}} dc & \text{(G4: } \beta > 0 \text{ \& } 1 - \alpha - 2\beta < 0) \end{cases}, \quad (43)$$

where $c_* = (4|\beta|/|1-\alpha-2\beta|)^{2/[3(1-\alpha+2\beta)]}$. Note that for $-1 \leq \alpha \leq 1$, if $\beta > 0$, we have $1-\alpha+2\beta > 0$, and if $\beta < 0$, we have $1-\alpha-2\beta > 0$. As $t \rightarrow t_s$, c approaches to its minimum value; $c \rightarrow c_*$ for G1 and G2, and $c \rightarrow 0$ for G3 and G4. We split the integration range into two parts as

$$\int_1^c [\dots] dc = \left(\int_1^{c_s} + \int_{c_s}^c \right) [\dots] dc, \quad \text{where } \int_1^{c_s} [\dots] dc \equiv t_s \text{ and } c_s = \begin{cases} c_* & \text{for G1 and G2} \\ 0 & \text{for G3 and G4} \end{cases}. \quad (44)$$

Therefore, Eq. (43) can be rewritten as

$$t - t_s = \begin{cases} \frac{1}{A_1} \int_{c_*}^c \sqrt{c} \left[\frac{1-\alpha-2\beta}{1-\alpha+2\beta} \left(c^{3(1-\alpha+2\beta)/2} - c_*^{3(1-\alpha+2\beta)/2} \right) \right]^{\frac{\alpha+2\beta}{1-\alpha-2\beta}} dc & \text{(G1)} \\ \frac{1}{A_1} \int_{c_*}^c \sqrt{c} \left[\frac{1-\alpha-2\beta}{|1-\alpha+2\beta|} \left(-c^{-3|1-\alpha+2\beta|/2} + c_*^{-3|1-\alpha+2\beta|/2} \right) \right]^{\frac{\alpha+2\beta}{1-\alpha-2\beta}} dc & \text{(G2)} \\ \frac{1}{A_1} \int_0^c \sqrt{c} \left[\frac{1-\alpha-2\beta}{1-\alpha+2\beta} \left(c^{3(1-\alpha+2\beta)/2} + c_*^{3(1-\alpha+2\beta)/2} \right) \right]^{\frac{\alpha+2\beta}{1-\alpha-2\beta}} dc & \text{(G3)} \\ \frac{1}{A_1} \int_0^c \sqrt{c} \left[\frac{1-\alpha-2\beta}{1-\alpha+2\beta} \left(-c^{3(1-\alpha+2\beta)/2} + c_*^{3(1-\alpha+2\beta)/2} \right) \right]^{\frac{\alpha+2\beta}{1-\alpha-2\beta}} dc & \text{(G4)} \end{cases}. \quad (45)$$

We perform the Taylor expansion for the term in the parentheses of the integrand about $c = c_*$ for G1 and G2 and keep the leading order. For G3 and G4, we set $c = 0$ in the parentheses and get the leading order of the integrand. Keeping the leading order, the integration gives, in the limit of $t \rightarrow t_s$,

$$c(t) \sim \begin{cases} c_* + \text{const.} \times (t - t_s)^{(1-\alpha-2\beta)} & \text{(G1 and G2)} \\ (t - t_s)^{2/3} & \text{(G3 and G4)} \end{cases}. \quad (46)$$

Using this result of c , we obtain d from Eq. (28),

$$d \sim \begin{cases} t - t_s & \text{(G1 and G2)} \\ (t - t_s)^{-1/3} & \text{(G3 and G4)} \end{cases}. \quad (47)$$

As a result, the three-volume density becomes

$$\mathcal{V}_3 \sim t - t_s \quad \text{(G1-G4)}, \quad (48)$$

the energy density becomes

$$\rho \sim \begin{cases} \frac{1}{(t-t_s)^{1+\alpha+2\beta}} & \text{(G1 and G2)} \\ \frac{1}{(t-t_s)^{1+\alpha-2\beta}} & \text{(G3 and G4)} \end{cases}, \quad (49)$$

and the Kretschmann scalar becomes

$$\mathcal{K} \sim \begin{cases} \frac{1}{(t-t_s)^{2(1+\alpha+2\beta)}} & \text{(G1 and G2)} \\ \frac{1}{(t-t_s)^4} & \text{(G3 and G4)} \end{cases}. \quad (50)$$

The behaviour of $\rho(t_s)$ and $\mathcal{K}(t_s)$ can be characterized by the regions in the α - β plane in Fig. 2. The regions are split by two lines S1 ($1 + \alpha + 2\beta = 0$) and S2 ($1 + \alpha - 2\beta = 0$).

- 1) In the region below S1, $\rho(t_s) = \mathcal{K}(t_s) = 0$ (e.g.: ii-B in Sec. IV C).
- 2) On S1, $\rho(t_s)$ and $\mathcal{K}(t_s)$ are finite (iii-C).
- 3) In the region between S1 and S2, $\rho(t_s)$ and $\mathcal{K}(t_s)$ diverge (i-A).
- 4) In the region above S2, $\rho(t_s) = 0$ and $\mathcal{K}(t_s)$ diverges (ii-A).
- 5) On S2, $\rho(t_s)$ is finite and $\mathcal{K}(t_s)$ diverges (iii-A).

Therefore, the initial singularity can be removed only on S1 and in the region below.

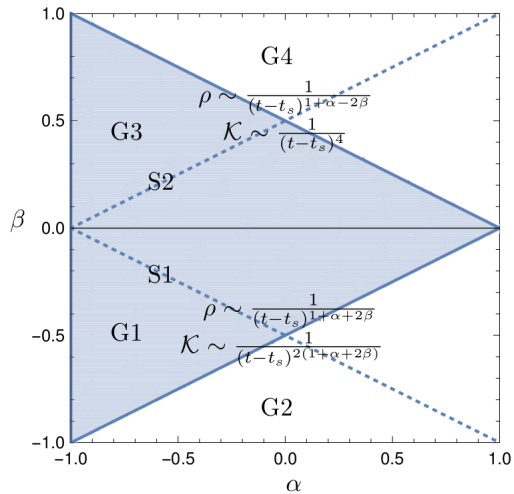


FIG. 2. Diagram for ρ and \mathcal{K} at $t \rightarrow t_s$ in α - β plane. Class G is split into four triangular regions by G1-G4. The shaded region ($1 - \alpha - 2|\beta| > 0$) consists of G1 and G3 divided by $\beta = 0$, and the unshaded region ($1 - \alpha - 2|\beta| < 0$) consists of G2 and G4. The dotted lines S1 and S2 represent $1 + \alpha + 2\beta = 0$ and $1 + \alpha - 2\beta = 0$, respectively. Note that the initial singularity can be removed on S1 and in the region below.

V. LATE TIME BEHAVIOUR

In this section, we investigate the late-time behaviour of the solutions at large t . We focus on different classes separately. We summarized the results in Fig. 3.

Class G: general class

As $t \rightarrow \infty$, we expect that the integration in Eq. (43) diverges. For Class G1 and G2, we observed from our calculations that the integration diverges as $c \rightarrow \infty$ and becomes finite as $c \rightarrow c_*$. For the class G3, the integration diverges also as $c \rightarrow \infty$. For the class G4, however, the integration diverges as $c \rightarrow c_*$.

After carrying out integrations, we find c at large t ,

$$c(t) \sim \begin{cases} t^{2(1-\alpha-2\beta)/[3(1-\alpha^2+4\beta^2)]} & (\text{G1 and G3}) \\ t^{2/3} & (\text{G2}) \\ c_* - \text{const.} \times t^{-|1-\alpha-2\beta|} & (\text{G4}) \end{cases} . \quad (51)$$

Using the results of c in the limit of $c \rightarrow \infty$, or $c \rightarrow c_*$, we obtain d from Eq. (28) as a function of c at large t ,

$$d \sim \begin{cases} c^{(1-\alpha+4\beta)/(1-\alpha-2\beta)} & (\text{G1 and G3}) \\ c^{-1/2} & (\text{G2}) \\ (c_* - c)^{-1/|1-\alpha-2\beta|} & (\text{G4}) \end{cases} . \quad (52)$$

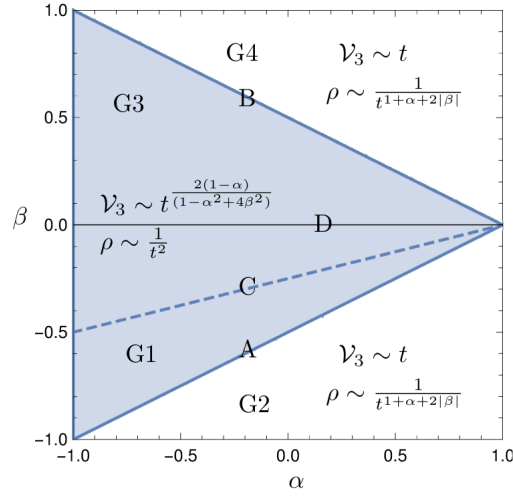


FIG. 3. Diagram for \mathcal{V}_3 and ρ at large t in α - β plane. The lower border between the shaded and the unshaded regions corresponds to Class A, and the upper border to Class B. The dashed line in G1 corresponds to Class C, and the solid horizontal line between G1 and G3 to Class D ($\beta = 0$: FRW). Considering the power in t , ρ evolves in the same manner with that of FRW in the shaded region, and decreases faster than that of FRW in the unshaded region. \mathcal{V}_3 increases slower than that of FRW in all regions.

The three-volume density becomes

$$\mathcal{V}_3 \sim \begin{cases} t^{2(1-\alpha)/(1-\alpha^2+4\beta^2)} & (\text{G1 and G3}) \\ t & (\text{G2 and G4}) \end{cases}. \quad (53)$$

The energy density becomes

$$\rho \sim \begin{cases} \frac{1}{t^2} & (\text{G1 and G3}) \\ \frac{1}{t^{1+\alpha+2|\beta|}} & (\text{G2 and G4}) \end{cases}. \quad (54)$$

Note that \mathcal{V}_3 diverges and ρ vanishes as $t \rightarrow \infty$. Class G1-G4 correspond to each rectangular triangle in Fig. 3.

Class C: $1 - \alpha + 4\beta = 0$ ($\alpha \neq 1$ and $\beta \neq 0$)

Imposing the same initial conditions with the Class G at $t = 0$, we have the same relation $A_2 = 3A_1$ from Eq. (35), but have $A_{3C} = 2$ from Eq. (36). Then Eq. (37) becomes

$$t = \frac{1}{A_1} \int_1^c c^{(3\alpha+1)/4} \left[3 - 2c^{-3(1-\alpha)/4} \right]^{\frac{3\alpha-1}{3(1-\alpha)}} dc. \quad (55)$$

This integration diverges as $c \rightarrow \infty$. Then from Eqs. (55) and (36), we have

$$c \sim t^{4/(3\alpha+5)}, \quad d = \text{const.} \quad (56)$$

The three-volume density and the energy density at large t are given by

$$\mathcal{V}_3 \sim t^{8/(3\alpha+5)}, \quad \rho \sim \frac{1}{t^2}. \quad (57)$$

Class C corresponds to the dashed line in Fig 3. Note that this class is contained in G1.

Class D: $\beta = 0$

(i) **FRW universe:** For this class, the metric is diagonal, and c and d were obtained in an exact form, Eq. (40). At large t , we have

$$c = d \sim \begin{cases} e^{A_1 t} & (\alpha = -1) \\ t^{2/[3(1+\alpha)]} & (\alpha \neq -1) \end{cases}. \quad (58)$$

The three-volume density and the energy density at large t are given by

$$\mathcal{V}_3 \sim \begin{cases} e^{3A_1 t} & (\alpha = -1) \\ t^{2/(1+\alpha)} & (\alpha \neq -1) \end{cases}, \quad \rho \sim \begin{cases} \text{const.} & (\alpha = -1) \\ \frac{1}{t^2} & (\alpha \neq -1) \end{cases}. \quad (59)$$

Class D corresponds to the horizontal axis in Fig. 3.

(ii) **Non-FRW universe:** For this class, the metric is non-diagonal, and c and d are given by Eqs. (38) and (39). However, we find that the late-time behaviours of \mathcal{V}_3 and ρ are the same as Class D-(i).

Class A ($1 - \alpha + 2\beta = 0$) and Class B ($1 - \alpha - 2\beta = 0$)

For Class A and B, it is difficult to obtain the solution at large t from directly integrating Eqs. (31) and (34). However, since Class A is the border of G1 and G2, and Class B is the border of G3 and G4 (i.e., the border lines between the shaded and unshaded regions in Fig. 3), we can deduce \mathcal{V}_3 and ρ . The conditions for Class A and B can be written as $1 - \alpha - 2|\beta| = 0$ which gives $2|\beta| = 1 - \alpha$. From Eqs. (53) and (54), we observe that the functional forms of \mathcal{V}_3 and ρ converge at the borders,

$$\mathcal{V}_3 \sim t, \quad \rho \sim \frac{1}{t^2}. \quad (60)$$

The behaviours of \mathcal{V}_3 and ρ at large t are summarized in the diagram in Fig. 3. Consider the power-law dependence of ρ and \mathcal{V}_3 on t . In the shaded region, ρ evolves in the same manner with that of FRW (Class D), while \mathcal{V}_3 exhibits a slower expansion than that of FRW. In the unshaded region, ρ exhibits a more rapid decrease than that of FRW, while \mathcal{V}_3 evolves linearly in t implying a slower expansion than that of FRW. Therefore, with off-diagonal stress, the expansion of \mathcal{V}_3 is slower, and ρ decreases more rapidly (at most equally) compared with the FRW universe.

The expansion of \mathcal{V}_3 can be explained by the Raychaudhuri equation which is

$$\dot{\Theta} + \frac{1}{3}\Theta^2 + \sigma^2 - \omega^2 + R_{\mu\nu}u^\mu u^\nu = 0. \quad (61)$$

We note from Sec. II that $\Theta = 2\dot{c}/c + \dot{d}/d = \dot{\mathcal{V}}_3/\mathcal{V}_3$ and $\sigma^2 = \sigma_{\mu\nu}\sigma^{\mu\nu} = 2(\dot{c}/c - \dot{d}/d)^2/3$. For the FRW universe ($\beta = 0$), $\sigma^2 = 0$ as $c = d$ always. However, the shear term is nonzero for $\beta \neq 0$. Therefore, the positive contribution from σ^2 makes the expansion Θ slower.

The behaviour of ρ can be explained by the conservation equation,

$$\dot{\rho} + \left(2\frac{\dot{c}}{c} + \frac{\dot{d}}{d}\right)(\rho + p) - 2\left(\frac{\dot{c}}{c} - \frac{\dot{d}}{d}\right)\sigma = 0. \quad (62)$$

At late times, the off-diagonal stress term behaves as

$$-2\left(\frac{\dot{c}}{c} - \frac{\dot{d}}{d}\right)\sigma \sim \begin{cases} \frac{|\beta|}{t^3} & \text{(G1 and G3)} \\ \frac{|\beta|}{t^{2+\alpha+2|\beta|}} & \text{(G2 and G4)} \end{cases}. \quad (63)$$

This term contributes negatively to the evolution of ρ , and make ρ decreases faster than in the FRW universe. As a whole, the energy density leaks to the shear stress, so drops faster. This makes the expansion of the Universe slower.

VI. ANISOTROPY

In this section, we discuss the anisotropy of our model. Since our model corresponds to the Bianchi type VII as seen from the metric (11), we define the anisotropy $H_d/H_c \equiv (\dot{d}/d)/(\dot{c}/c)$. It is plotted in Fig. 4. Depending on the values of parameters, the initial anisotropy decreases from a large value, or increases from a small value. At late times, however, the anisotropy approaches a constant value except for the class G4. The asymptotic value of the anisotropy can be evaluated at late times from Eqs. (51) and (52),

$$\frac{H_d}{H_c} \sim \begin{cases} \frac{1-\alpha+4\beta}{1-\alpha-2\beta} & \text{(G1 and G3)} \\ -\frac{1}{2} & \text{(G2)} \\ \frac{1}{|1-\alpha-2\beta|} \left(-1 + \frac{c_*}{\text{const.}} t^{|1-\alpha-2\beta|}\right) & \text{(G4)} \end{cases}. \quad (64)$$

Since the anisotropy is due to the off-diagonal stress, its magnitude is not negligible unless β is small. The situation is different from the rapid decay of anisotropy with a cosmological constant in the background [14].

At late times, one can check from Eqs. (51) and (52) that $H_c > 0$ in all the regions of the diagram in Fig. 3 and $H_d > 0$ only in the region above the line C. It means d exhibits a contraction at late times in the region below the line C.

Let us discuss some limits of the parameters. For the late-time solutions in G1 and G3, let us expand H_c and H_d about two equation-of-state parameters at $\alpha = -1$ (to explain current observational acceleration) and $\beta = 0$ (to have small anisotropy),

$$H_c \approx \frac{2}{3(1+\alpha)t} \left[1 - \beta \left(1 + \frac{2\beta}{1+\alpha} \right) + \dots \right], \quad (65)$$

$$H_d \approx \frac{2}{3(1+\alpha)t} \left[1 + 2\beta \left(1 - \frac{\beta}{1+\alpha} \right) + \dots \right]. \quad (66)$$

In these parameter expansions, the anisotropy, i.e., the difference in H_c and H_d starts to appear in the second-leading order. The expansions of spacetime with these parameter ranges ($\alpha \approx -1$ and $\beta \approx 0$) may

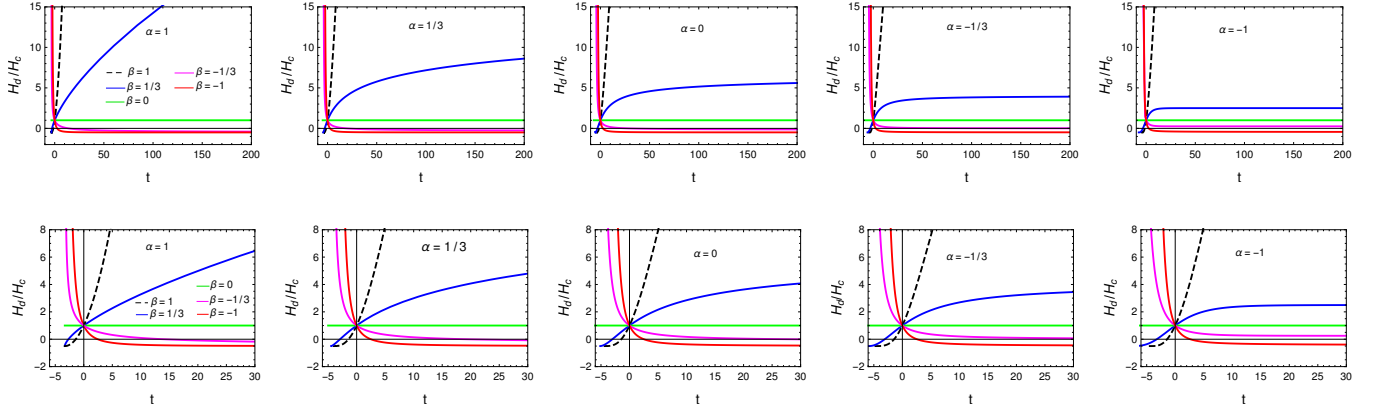


FIG. 4. Plots of H_d/H_c . (Lower panel is for zoom-in plots.) At late times, the anisotropy approaches a constant except for G4. The anisotropy is large unless β is small. The negative value at late times indicates the contraction of d , which occurs in the region below the line C in the diagram of Fig. 3.

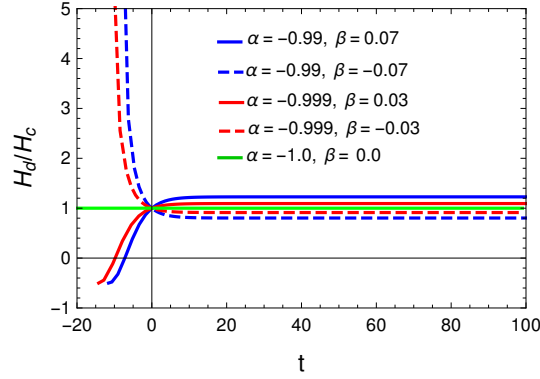


FIG. 5. Plots of H_d/H_c for several values of α and β near $\alpha = -1$ and $\beta = 0$. The anisotropy is large at early times, and small at late times.

give some hints for explaining the current acceleration of the Universe with a negligible anisotropy. However, these ranges mimic the cosmological constant, so the evolution of the Universe will not be explained solely by the fluid; we need other matter contents to explain the currently observed universe. On the contrary, at early times, the anisotropy is large in these parameter ranges (see Fig. 5). This may also give some hints for the observed anisotropy in the early universe. This needs more investigation, but is beyond the scope of this work.

VII. CONCLUSIONS

We investigated the effect of the off-diagonal stress tensor in the evolution of the spacetime. The energy-momentum tensor of the matter fluid consists of the energy density, the pressure, and the off-diagonal stress components. We considered each component of the pressure and the stress having the same value respectively

with introducing the off-diagonal spatial metric components of the same value. (With a suitable coordinate transformation, the set-up can be put into the Bianchi type VII anisotropic spacetime.) We assumed the simplest equation of states for which the pressure and the off-diagonal stress are proportional to the energy density, $p = \alpha\rho$ and $\sigma = \beta\rho$.

We solved the Einstein's equation with the off-diagonal spatial components of the metric turned on. One of the metric functions is given by an implicit integral form which we could solve numerically. We solved the field equations for the range of parameters, $-1 \leq \alpha, \beta \leq 1$. Depending on the values of the parameters, the integration of the field equation was classified into five types.

The solutions of all the classes exhibit the initially vanishing volume except for the pure de Sitter ($\alpha = -1, \beta = 0$), which means that the three-volume density \mathcal{V}_3 is zero at the initial moment t_s . \mathcal{V}_3 increases afterwards.

The evolution pattern of the energy density ρ at the early stage varies depending on the parameters. For some cases, ρ drops from infinity as the usual Friedmann universe ($\beta = 0$). For others, however, ρ starts from a finite value and increases/decreases at the early stage. At late times, ρ decreases for all classes except for the pure de Sitter. At late times, we could derive the asymptotic solutions analytically. They exhibit that ρ decreases faster than, or at most equal to the usual Friedmann universe considering the power of t -dependence.

Although the three-volume density vanishes at the initial moment, $\mathcal{V}_3(t_s) = 0$, the curvature is not always divergent. We analysed the energy density and the Kretschmann curvature (\mathcal{K}) near the initial moment t_s . We found that $\rho(t_s) = 0$ and $\mathcal{K}(t_s) = 0$ for the parameters in the range, $1 + \alpha + 2\beta < 0$, so the big-bang singularity can be removed. We observed that the weak-energy condition is violated in this range. Note that this is achieved when the off-diagonal stress is quite significant, i.e., the value of β is not very close to zero.

As a whole, introducing the off-diagonal stress in fluid, the energy density transfers to the stress. This makes the energy density drops faster than the usual stress-free universe (FRW), and the expansion of the Universe becomes slower as a result.

Our model exhibits an anisotropic evolution of spacetime as a Bianchi type VII. At late times, the anisotropy settles down to a constant value except for $1 - \alpha - 2\beta < 0$. The anisotropy is not small unless the off-diagonal stress is negligible, $\beta \approx 0$. With $\alpha \approx -1$ and $\beta \approx 0$, our model may provide a clue to explain the acceleration of the current universe and the dipole anisotropy in the early universe although other matter contents are necessary to be complete. Further investigations are necessary for this.

Acknowledgements

Authors are grateful to Hyeong-Chan Kim, Wonwoo Lee, and Byungchan Kim for useful discussions. This work was supported by the grant from the National Research Foundation funded by the Korean government, No. NRF-2020R1A2C1013266.

-
- [1] O. M. Pimentel, G. A. González and F. D. Lora-Clavijo, “The Energy-Momentum Tensor for a Dissipative Fluid in General Relativity,” *Gen. Rel. Grav.* **48**, no.10, 124 (2016) [arXiv:1604.01318 [gr-qc]].
 - [2] R. Maartens, “Causal thermodynamics in relativity,” [arXiv:astro-ph/9609119 [astro-ph]].
 - [3] W. Misner, K. S. Thorne, and J. A. Wheeler, “Gravitation,” (Princeton University Press, USA, 2017).
 - [4] S. Bravo Medina, M. Nowakowski and D. Batic, “Viscous Cosmologies,” *Class. Quant. Grav.* **36**, no.21, 215002 (2019) [arXiv:1901.09787 [gr-qc]].
 - [5] A. K. Banerjee and N. O. Santos, “Spatially Homogeneous Cosmological Models,” *Gen. Rel. Grav.* **16**, no.03, 217-224 (1984)
 - [6] A. Banerjee, S. B. Duttachoudhury and A. K. Sanyal, “Bianchi type I cosmological model with a viscous fluid,” *J. Math. Phys.* **26**, 3010-3015 (1985) [arXiv:2103.07342 [gr-qc]].
 - [7] O. Gron, “Viscous Inflationary Universe Models,” *Astrophys. Space Sci* **173**, 191-225 (1990)
 - [8] A. Banerjee, A. K. Sanyal and S. Chakrabarty, “Bianchi II, VIII and IX viscous fluid cosmology,” *Astrophys. Space Sci.* **166**, 259-268 (1990) [arXiv:2105.10696 [gr-qc]].
 - [9] T. Singh and R. Chaubey, “Bianchi type-V universe with a viscous fluid and Λ -term,” *Pramana* **68**, 721-734 (2007)
 - [10] S. Weinberg, “Gravitation and Cosmology: Principles and Applications of the General Theory of Relativity,” John Wiley and Sons, 1972.
 - [11] R. M. Wald, “General Relativity,” Chicago University Press, 1984.
 - [12] G. F. R. Ellis, “Dynamics of pressure free matter in general relativity,” *J. Math. Phys.* **8**, 1171-1194 (1967).
 - [13] J. M. Stewart and G. F. R. Ellis, “Solutions of Einstein’s equations for a fluid which exhibit local rotational symmetry,” *J. Math. Phys.* **9**, 1072-1082 (1968).
 - [14] R. M. Wald, “Asymptotic behavior of homogeneous cosmological models in the presence of a positive cosmological constant,” *Phys. Rev. D* **28**, 2118-2120 (1983).